COLENS, A., DECLERCQ, J. P., GERMAIN, G., PUTZEYS, J. P. & VAN MEERSSCHE, M. (1974). *Cryst. Struct. Commun.* **3**, 119-122.
DECLERCQ, J. P., GERMAIN, G. & WOOLFSON, M. M. (1975). *Acta Cryst.* A**31**, 367-372.
DECLERCQ, J. P., GERMAIN, G. & WOOLFSON, M. M. (1979). *Acta Cryst.* A**35**, 622-626.
DE TITTA, G. T., EDMONDS, J. W., LANGS, D. A. & HAUPTMAN, H. (1975). *Acta Cryst.* A**31**, 472-479.
GIACOVAZZO, C. (1976). *Acta Cryst.* A**32**, 91-99.
HOEKSTRA, A., VOS, A., BRAUN, P. B. & HORNSTRA, J. (1975). *Acta Cryst.* B**31**, 1708-1715.
HOVESTREYDT, E., KLEPP, K. & PARTHÉ, L. (1983). *Acta Cryst.* C**39**, 422-425.
ITO & NOVACKI (1974). *Z. Kristallogr.* **139**, 85-102.
JONES, P. G., SHELDRICK, G. M., GLÜSENKAMP, K.-H. & TIETZE, L. F. (1980). *Acta Cryst.* B**36**, 481-483.
KARLE, I. L. & KARLE, J. (1981). *Proc. Natl Acad. Sci. USA*, **78**, 681-685.
KARLE, J. & KARLE, I. L. (1966). *Acta Cryst.* **21**, 849-859.
MAIN, P. (1977). *Acta Cryst.* A**33**, 750-757.
NGUYEN-HUY DUNG, VO-VAN TIEN, BEHM, H. J. & BEURSKENS, P. T. (1987). *Acta Cryst.* C**43**, 2258-2260.
OVERBEEK, A. R. & SCHENK, H. (1976). *Proc. K. Ned. Akad. Wet. Ser. B*, **79**, 341-343.
SCHENK, H. (1974). *Acta Cryst.* A**30**, 477-481.
SHELDRICK, G. M., DAVISON, B. E. & TROTTER, J. (1978). *Acta Cryst.* B**34**, 1387-1389.
SHELDRICK, G. M. & TROTTER, J. (1978). *Acta Cryst.* B**34**, 3122-3124.
SUCK, D., MANOR, P. C. & SAENGER, W. (1976). *Acta Cryst.* B**32**, 1727-1737.
WALLWORK, S. C. & POWELL, H. M. (1980). *J. Chem. Soc. Perkin Trans.* 2, 641-646.
WHITE, P. & WOOLFSON, M. M. (1975). *Acta Cryst.* A**31**, 53-56.
YAO, J. (1981). *Acta Cryst.* A**37**, 642-644.

Acta Cryst. (1992). A**48**, 865-872

Modeling the Diffraction Process of Molecular Crystals: Computation of X-ray Scattering Intensities from *Ab Initio* Electron Densities

BY H. BRUNING AND D. FEIL

Chemical Physics Laboratory, University of Twente, POB 217, 7500 *AE Enschede, The Netherlands*

(*Received* 1 *October* 1991; *accepted* 15 *April* 1992)

Abstract

An algorithm for calculating the scattering factors of atomic fragments in molecules as defined by the Stockholder recipe is presented. This method allows the calculation, from *ab initio* molecular wave functions, of structure factors including individual anisotropic atomic temperature factors. These structure factors agree with the model used in most least-squares multipole-refinement procedures. Calculations on the H_2O molecule illustrate the method.

1. Introduction

X-ray scattering experiments can provide us with a large amount of information on the structures of molecular crystals. Accurate high-resolution experiments can even reveal details of the electron-density distribution, such as bonding densities and subtle effects of intermolecular interactions and polarization by the crystal field (Krijn, Graafsma & Feil, 1988; Krijn & Feil, 1988). This fact makes it relevant to calculate in advance the results of an X-ray scattering experiment by quantum-chemical *ab initio* methods. Firstly, it gives us the possibility to verify experimentally the approximations used in *ab initio* calculations of the electron-density distribution in a crystal. Is it necessary to use the Bloch-function approach in crystal calculations or do cluster calculations suffice? When a cluster approach is deemed suitable one can test the basis-set truncation error and the approximations that have to be used to incorporate the embedding of the cluster in the crystal, *i.e.* the polarization by the electrostatic crystal field and the effect of the exchange repulsion by the surrounding molecules. This is particularly important when hydrogen bonds and electrostatic fields are included in the calculation on molecular crystals. Secondly, the theoretically calculated X-ray intensities can be used to check the crystallographic refinement procedures that are applied to remove noise from the data and to obtain information on the electron-density distribution in analytic form. In particular, one can verify whether the structural data on which the theoretical calculations are based are reproduced by the refinement.

Most experimental X-ray diffraction data on crystals are interpreted with a model based on the assumption that the crystal is built up of atoms. The lattice vibrations of the crystal, which consist of zero-point vibrations and thermal excitations, are taken into account by the Debye-Waller factor. Widely used expressions of the Debye-Waller factor are based on the assumption that the atoms behave as coupled harmonic oscillators. This harmonic-vibration model implies that the density distribution for each nucleus is given by a three-dimensional Gaussian distribution. The adiabatic approximation leads to the model of

0108-7673/92/060865-08$06.00

rigid following, *i.e.* the time-averaged density distribution of the electrons of the atom is the convolution of the static atomic electron-density distribution with the Gaussian nuclear distribution. It can be shown that the time-averaged X-ray scattering intensities are well approximated by the radiation intensities scattered by the time-averaged electron distribution (Stewart & Feil, 1980). Routine analyses of X-ray data are usually based on the assumption of spherical atoms. This limits the structural information of single crystals to atomic positions and thermal-displacement parameters. The model lacks the effects of the distortion of the atomic electron density distribution by the chemical bonds and the polarization by the crystal field. In a more sophisticated model the nonspherical part of the atomic density is expanded into an atom-centered basis set of multipole functions. The expansion coefficients are parameters in the least-squares refinement (Stewart, 1976; Hirshfeld, 1977*a*; Hansen & Coppens, 1978). To obtain a good description of the difference-density distribution by a limited basis set, one has to use rather diffuse functions that reach well into the regions occupied by neighboring atoms. The assignment of all electron density described by a deformation function to the atom on which it is centered is an arbitrary partitioning of the electron-density distribution that is hard to reconcile with the assumption of rigid following.

The electron-density distribution in molecules can be calculated very accurately by quantum-chemical methods like the Hartree–Fock SCF-LCAO or the density-functional methods. These quantum-chemical methods do not include the effects of thermal motion on the electron-density distribution. Even the application of the Born–Oppenheimer approximation does not make it feasible to account properly for internal vibrations since this would require the calculation of the electron wave function for many nuclear configurations. Hence, one cannot compare the Fourier transform of the theoretically obtained electron-density distribution with the experimental X-ray structure factors. When applying the Debye–Waller formalism, one meets the problem of partitioning the electron-density distribution into atomic fragments. This problem is simple in the case of monoatomic crystals like silicon (Velders & Feil, 1989). In the case of molecular crystals it can be avoided by neglect of internal motion and restriction to rigid-body motion only (Stevens, Rys & Coppens, 1977). In the presence of strong molecular interaction, however, as is the case with short intermolecular hydrogen bonds, the rigid-body model gives a poor description of thermal motion.

Several methods of dividing a molecule into atomic parts have been proposed. The widely used Mullikan population analysis is based on a partitioning of the one-electron density matrix into atomic submatrices. The results of the method vary greatly with the basis set used in the *ab initio* calculation. Because of this basis-set dependence it is not suitable for our purpose. Another method has been proposed by Bader, Beddall & Cade (1971). It is based on the topological properties of the crystalline electron-density distribution and divides the molecule into sharply bounded atomic regions. The calculation of the structure factor requires the Fourier transform of the electron-density distribution. For sharply bounded atoms this can only be achieved by cumbersome three-dimensional windowing techniques. This computational problem makes the method very unattractive. The effect of boundaries on the scattering factor is discussed in the Appendix.

Here we propose a scheme that is based on the Stockholder partitioning (Hirshfeld, 1977*b*). Since the Stockholder atoms possess fuzzy boundaries there is no problem of windowing. To the scattering factor of each Stockholder atom we apply a Debye–Waller factor. We also give an algorithm by which the scattering factor of the *ab initio* nonspherical atom can be calculated on a computer.

2. Computational method

The method requires that the electron-density distribution ρ of a molecule has been calculated at points $\mathbf{r}$ on a specific grid by some (quantum-chemical) method. The grid is chosen as described below.

The electron-density distribution of a molecule can be expressed in two parts,

$$\rho(\mathbf{r}) = \rho(\mathbf{r})_{\rm pro} + \Delta\rho(\mathbf{r}), \tag{1}$$

where $\rho_{\rm pro}(\mathbf{r})$, the promolecule electron-density distribution, is defined as the sum of the localized spherical atomic density distributions $\rho_i^0(\mathbf{r})$,

$$\rho_{\rm pro}(\mathbf{r}) = \sum_i \rho_i^0(\mathbf{r}-\mathbf{R}_i). \tag{2}$$

$\Delta\rho(\mathbf{r})$ is the difference density due to chemical bonding. In the absence of $\Delta\rho(\mathbf{r})$, partitioning becomes trivial,

$$\rho_j^0(\mathbf{r}-\mathbf{R}_j) = [\rho_j^0(\mathbf{r}-\mathbf{R}_j)/\rho_{\rm pro}(\mathbf{r})]\rho_{\rm pro}(\mathbf{r}). \tag{3}$$

Hirshfeld's Stockholder method applies the same partitioning scheme to $\Delta\rho(\mathbf{r})$,

$$\Delta\rho_j(\mathbf{r}) = [\rho_j^0(\mathbf{r}-\mathbf{R}_j)/\rho_{\rm pro}(\mathbf{r})]\Delta\rho(\mathbf{r}). \tag{4}$$

The atomic scattering factor is then

$$f_j(\mathbf{k}) = \mathcal{F}[\rho_j^0(\mathbf{r}) + \Delta\rho_j(\mathbf{r}+\mathbf{R}_j)]. \tag{5}$$

The first term of the Fourier transform can be calculated by standard methods from atomic wave functions (McWeeney, 1951). In general there will be no analytical expression for the Fourier transform of $\Delta\rho_j$. We present a scheme that only requires the ability to compute $\Delta\rho_j(\mathbf{r})$ at any given point $\mathbf{r}$. The first step is

to expand $\Delta\rho_j(\mathbf{r})$,

$$\Delta\rho_j(\mathbf{r}) = \sum_{n=0}^{\infty}\sum_{l=0}^{\infty}\sum_{m=-l}^{l} c_{nlm,j} S_{lm}(\theta,\varphi) L_n^l(\alpha_{l,j}r)(\alpha_{l,j}r)^l \times \exp(-\alpha_{l,j}r), \quad (6)$$

where $L_n^l(\mathrm{r})$ are associated Laguerre polynomials and $S_{lm}(\theta,\varphi)$ are real spherical harmonics. For practical purposes, the infinite series in (6) can be truncated at $n=8$ and $l=4$. The $\alpha_{l,j}$ in (6) are arbitrary positive constants that can be adjusted so as to minimize the effect of the series truncation. The accuracy of the expansion (6) is illustrated in Fig. 1.

From the orthogonality properties of the spherical harmonics,

$$\int_0^{\pi} d\theta \int_0^{2\pi} d\varphi \sin(\theta) S_{lm}(\theta,\varphi) S_{l'm'}(\theta,\varphi) = \delta_{ll'}\delta_{mm'}, \quad (7)$$

and of the associated Laguerre polynomials,

$$\int_0^{\infty} dr\, L_n^l(r) L_{n'}^l(r) r^l \exp(-r) = [(n+l)!/n]\delta_{nn'}, \quad (8)$$

where δ is the Kronecker delta function, the coefficients $c_{nlm,j}$ in (6) are given by

$$c_{lmn,j} = \frac{\alpha_{l,j} n!}{(n+l)!} \int_0^{\infty} dr \int_0^{\pi} d\theta \int_0^{2\pi} d\varphi \sin(\theta) \times S_{lm}(\theta,\varphi) L_n^l(\alpha_{l,j}r) \Delta\rho_j(\mathbf{r}). \quad (9)$$

The integrals in (9) can be evaluated with high accuracy by numerical integration. The angular coordinate θ appears in the integrand of (9) as a product of associated Legendre functions of $\cos\theta$, explicitly as $L_n^l(\alpha_{l,j}r)$ and implicitly in $\Delta\rho_j(\mathbf{r})$. Therefore, the θ integration can be carried out by Gauss-Legendre quadrature in $\cos\theta$. The products of $\sin m\varphi$ and $\cos m\varphi$ can be integrated exactly on a regular grid in φ. The integration over r can be carried out exactly by Gauss-Laguerre quadrature in $\alpha_{l,j}r$. However, this has the disadvantage that, for each value of $\alpha_{l,j}$, a different integration grid for r has to be used. During the optimization of $\alpha_{l,j}$, the global minimum of the mean square error in the expansion is located by scanning over values of $\alpha_{l,j}$ and then the value of $\alpha_{l,j}$ is refined to reach the true minimum. For each value of $\alpha_{l,j}$ encountered in the optimization process the integral in (9) has to be evaluated. The calculation of $\Delta\rho_j(\mathbf{r})$ is very time consuming so much computer time can be saved when one integration grid in r is used for all values of $\alpha_{l,j}$. A typical r dependence of $\Delta\rho_j$ is shown in Fig. 2. From this curve it is clear that the integration can be limited to the interval from 0 to 5 Å. The curve shows regions in which the value changes greatly. First we recognize the core region in which the curve steeply ascends. The next region contains most of the valence density in which the curve is much less steep. The third region is the diffuse part of the density in which the curve is almost flat. To reach sufficient accuracy we integrated separately in five intervals: one in the core region, two in the valence region and two in the diffuse region; in each region, eight-point Gauss-Legendre quadrature was used. When the series in (6) is evaluated up to at least $n=2$, the electrostatic moments of the Stockholder atom are retained in the expansion.

The second step is to calculate the Fourier transform of (6). Equation (6) may be rewritten as

$$\Delta\rho_j(\mathbf{r}) = \sum_{n=0}^{\infty}\sum_{l=0}^{\infty}\sum_{m=-l}^{l} c'_{nlm,j} S_{lm}(\theta,\varphi) r^{n+l} \exp(-\alpha_{l,j}r) \quad (10)$$

and the Fourier transform of each term of (10) is given by

$$f_{nlm,j}(\mathbf{k}) = \int S_{lm}(\theta,\varphi) r^{n+l} \exp(-\alpha_{l,j}r) \exp(i\mathbf{k}\cdot\mathbf{r})\, d\mathbf{r}. \quad (11)$$

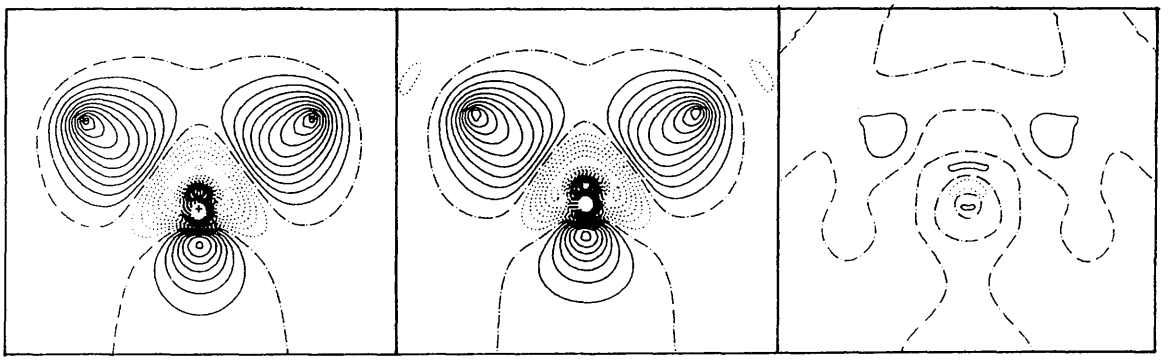

(a) (b) (c)

Fig. 1. Difference density of H_2O (*a*) from *ab initio* Hartree-Fock 6-31g**; (*b*) using the expansion (6); (*c*) error in expansion: (*b*) − (*a*). Contour interval (*a*), (*b*) 0.1 e Å^{-3}; (*c*) 0.05 e Å^{-3}.

The integral in (11) can be evaluated as pointed out by Stewart (1980). We make use of the expansion into spherical coordinates of a three-dimensional wave (Arfken, 1985):

$$\exp(i\mathbf{k}\cdot\mathbf{r}) = 4\pi(\pi/2rk)^{1/2} \sum_{p=0}^{\infty} i^p J_{p+1/2}(kr) \times \sum_{q=-p}^{p} Y^*_{pq}(\theta_r, \varphi_r)\, Y_{pq}(\theta_k, \varphi_k), \quad (12)$$

where $J_{p+1/2}(r)$ is a Bessel function and $Y_{pq}(\theta, \varphi)$ is a spherical harmonic. Substitution of (12) into (11) and application of the orthogonality properties of spherical harmonics yields

$$f_{nlm,j}(\mathbf{k}) = 4\pi i^l S_{lm}(\theta_k, \varphi_k) \int_0^{\infty} r^{n+l+2}(\pi/2rk)^{1/2} \times J_{l+1/2}(kr) \exp(-\alpha_{l,j} r)\, dr. \quad (13)$$

To solve the integral in (13) we use (Ryshik & Gradshteyn, 1965)

$$\int_0^{\infty} r^{l+1}(\pi/2rk)^{1/2} J_{l+1/2}(kr) \exp(-\alpha_{l,j} r)\, dr = (2k)^l l!/(\alpha_{l,j}^2 + k^2)^{l+1}. \quad (14)$$

The power of r on the left hand side of (14) can be raised to the desired value by differentiating (14) with respect to $-\alpha_{l,j}$. The final result is the scattering factor of a Stockholder atom:

$$f_j(\mathbf{k}) = f_j^0(\mathbf{k}) + \sum_{n=0}^{\infty} \sum_{l=0}^{\infty} \sum_{m=-l}^{l} c'_{nlm,j} f_{nlm,j}(\mathbf{k}). \quad (15)$$

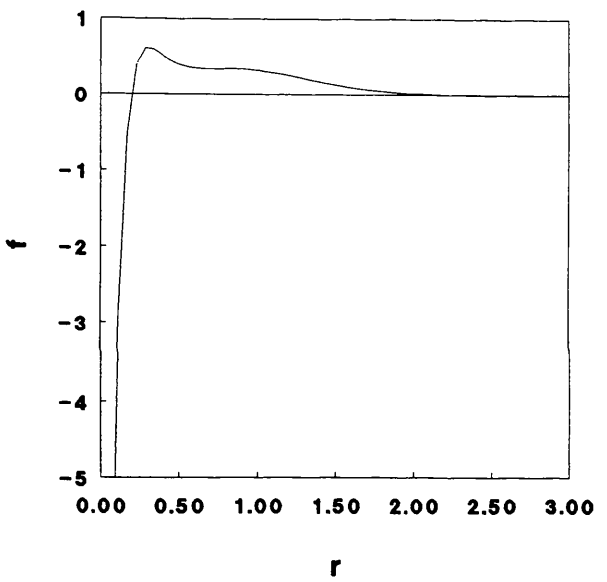

Fig. 2. Radial dependence of the difference-density function of an atom in the water molecule for $l=0$, $m=0$, computed from *ab initio* Hartree-Fock 6-31g**, atomic units.

Table 1. *Atomic isotropic thermal displacement parameters in* H_2O: $\langle u^2 \rangle$ (Å^2)

Temperature (K)	Atom O	Atom H
0	0.0000	0.0000
100	0.0121	0.0289
300	0.0256	0.0400

The next step, which leads to the crystal structure factor, is to multiply the nonspherical atomic scattering factor given by (15) by the atomic thermal displacement factor and to sum over all atoms in the asymmetric unit. Symmetry operations so as to cover the unit cell are applied in the usual way.

3. Application to the water molecule

To illustrate our method we have calculated structure factors for a water molecule (in the experimental gas-phase equilibrium geometry) placed in a large unit cell ($a=b=c=10$ Å, $\alpha=\beta=\gamma=90°$). The O atom is situated at the origin. The electron-density distribution of the isolated molecule was calculated by the Hartree-Fock-Slater $X\alpha$ discrete variational method (DVM) (Baerends, Ellis & Ross, 1973; Baerends & Ross, 1973; Baerends, Vernooys, Roozendaal, Boerrigter, Krijn, Feil & Sundholm, 1985) using a triple-zeta Slater-type basis set augmented with *d*- and *p*-polarization functions. The electron-density distribution of the water molecule is partitioned into atomic fragments according to the Stockholder recipe. The scattering factors of the atomic fragments are calculated in the way described in the previous section. Individual atomic thermal-displacement parameters corresponding to 0, 100 and 300 K (see Table 1) are applied to the atomic scattering factors. The values of the thermal-displacement parameters are based on the work of Eriksson & Hermansson (1983). The atomic scattering factors are added with appropriate phases to yield the Fourier transform of the electron-density distribution of the water molecule.

In experimental electron-density distribution studies, the influence of the difference-electron-density distribution on the structure factor is of interest. For the water molecule, the Fourier transform of $\Delta\rho(\mathbf{r})$ is plotted in Fig. 3. The figure shows a large peak at the origin, *i.e.* at low scattering angles, which are not accessible by X-ray diffraction. The figure shows two peaks in the regions in reciprocal space corresponding to waves in the direction of the O–H bonds. They represent the accumulation of charge in the bonding regions. These peaks are in the $(\sin\theta)/\lambda$ range that can be explored by X-ray diffraction. In this part of the reciprocal space, the thermal motion has a significant influence on the structure factor. This is illustrated in Fig. 4, which contains maps of Fourier syntheses for three different temperatures

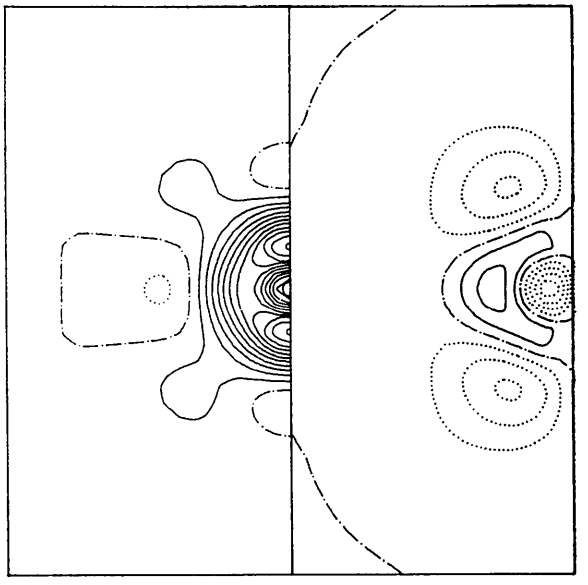

(a) (b)

Fig. 3. Scattering factor of the difference-density distribution of water in the plane of the molecule, $(\sin\theta)/\lambda < 1.0$ Å^{-1}, contour interval 0.05 e. (*a*) Real part; (*b*) imaginary part.

(0, 100 and 300 K) with series truncations at three different values of $(\sin\theta)/\lambda$ (0.8, 1.1 and 1.4 Å^{-1}). The dynamic electron-density distribution of the thermally vibrating water molecule has been analyzed by Hermansson (1983). For 0 K and truncation at 0.8 Å^{-1}, smooth contours appear in the bond and lone-pair regions. With truncation at higher angles, some details of the electron-density distribution in the O-atom core region can be seen and the contours in the bonding region are modified by the high-angle contributions. Therefore, to reach convergence of the Fourier synthesis, one has to include data at much higher angles. At 100 K, no more details of the atom core region can be seen, even when truncating at 1.4 Å^{-1}. At 300 K, even the bond and lone-pair features become weak.

Figs. 3 and 4 imply that only a limited amount of information on the electron-density distribution can be obtained by X-ray diffraction. Underneath the distinct peaks in a Fourier map there is a diffuse pattern of charge redistribution that is represented by a few low-angle reflections. In a least-squares refinement using a multipole model, this diffuse part of the difference-electron-density distribution

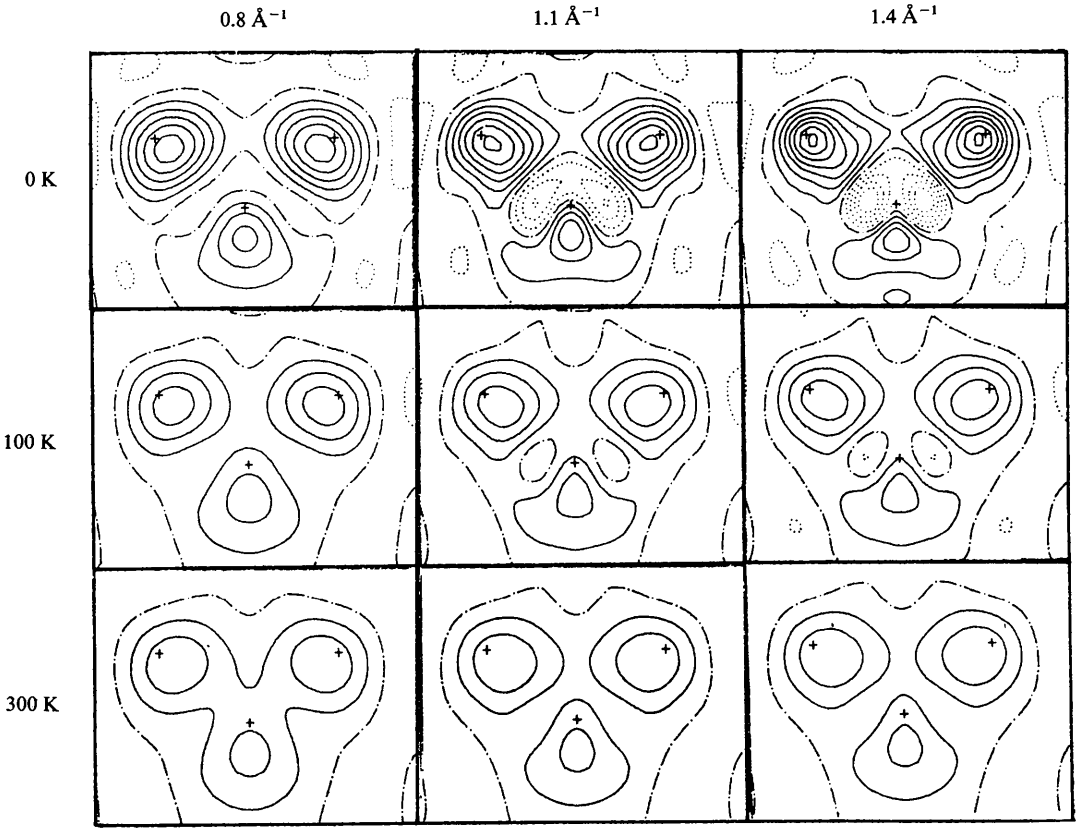

Fig. 4. Fourier syntheses of the difference-density distribution of water at three temperatures and three cutoff values in $(\sin\theta)/\lambda$, contour interval 0.1 e Å^{-3}.

provides only a small contribution to the sum of squares owing to the low scattering power of that density and to the small number of low-order reflections. Consequently, the value of the diffuse density is subject to large errors. For three sets of structure factors, one without thermal motion and the others at 100 and 300 K, we have performed multipole refinements with respect to $|F|$, with unit weights, using the LSEXP model (Hirshfeld, 1977*a*). Structure factors up to $(\sin\theta)/\lambda = 1.4$ Å^{-1} were included in the refinement. The refinements resulted in unweighted R factors that were less than 0.002. The resulting static electron-density distribution calculated from the multipole functions is plotted in Fig. 5. Comparison of Fig. 5 with Fig. 1 shows that the multipole refinement succeeds well in the deconvolution of the thermal smearing. The differences in the bond and lone-pair regions of the static maps are very small. The main difference is in the region near the atom nucleus: owing to truncation at $(\sin\theta)/\lambda = 1.4$ Å^{-1}, the polarization of the atom core is completely lost in the static maps.

4. Concluding remarks

We developed a method to calculate X-ray structure factors from an *ab initio* electron-density distribution that includes the rigid following model of thermal motion. The molecular-electron-density distribution is partitioned into atomic fragments according to the Stockholder recipe. The Fourier transform of the electron-density distribution of the Stockholder atom can be expressed analytically by a series.

The contribution of the difference-electron-density distribution to the X-ray scattering factor is calculated in the case of the water molecule. The difference-electron-density distribution can be recovered by a Fourier synthesis. A multipole refinement leads to a successful deconvolution of the thermal motion. These results show some of the limitations of X-ray electron-density-distribution studies. Neither the diffuse regions of intermolecular electron-density distributions nor the core regions of the atoms are accessible for experimental X-ray diffraction studies.

APPENDIX

The scattering factor of 'atoms in molecules': N in N_2

According to the 'theory of atoms in molecules' (Bader, Beddall & Cade, 1971), the N atoms in N_2 are separated by a plane that is, by symmetry, the σ_h plane. The nuclei are at the positions $(0, 0, -R/2)$ and $(0, 0, R/2)$. The electron-density distribution of the second atom is related to the electron-density distribution of the molecule by a step function:

$$\rho_N(\mathbf{r}) = \rho_{N_2}(\mathbf{r})\vartheta_z(\mathbf{r}), \qquad (A1)$$

$$\vartheta_z(\mathbf{r}) \equiv \begin{cases} 1, & z > 0 \\ 1, & z < 0. \end{cases} \qquad (A2)$$

The scattering factor of the N atom is given by the Fourier transform of (*A*1) with a phase factor added to displace the origin at the nuclear position. According to the convolution theorem of Fourier analysis, this results in

$$F_N(\mathbf{k}) = \exp(i\mathbf{k}\cdot\mathbf{R}/2)(2\pi)^{-3}\int \mathbf{du} F_{N_2}(\mathbf{k}-\mathbf{u})\Theta_z(\mathbf{u}), \qquad (A3)$$

where $\mathbf{R}$ denotes $(0, 0, R)$ and $\Theta_z(\mathbf{k})$ is the Fourier transform of $\vartheta_z(\mathbf{r})$, given by

$$\Theta_z(\mathbf{k}) = (2\pi)^2\delta(k_x)\delta(k_y)\lim_{\varepsilon\to 0}[i/(k_z + i\varepsilon)], \qquad (A4)$$

where $\delta(k)$ represents the Dirac delta function. Since we are interested here in the effect of introducing sharp boundaries rather than in the effect of bonding,

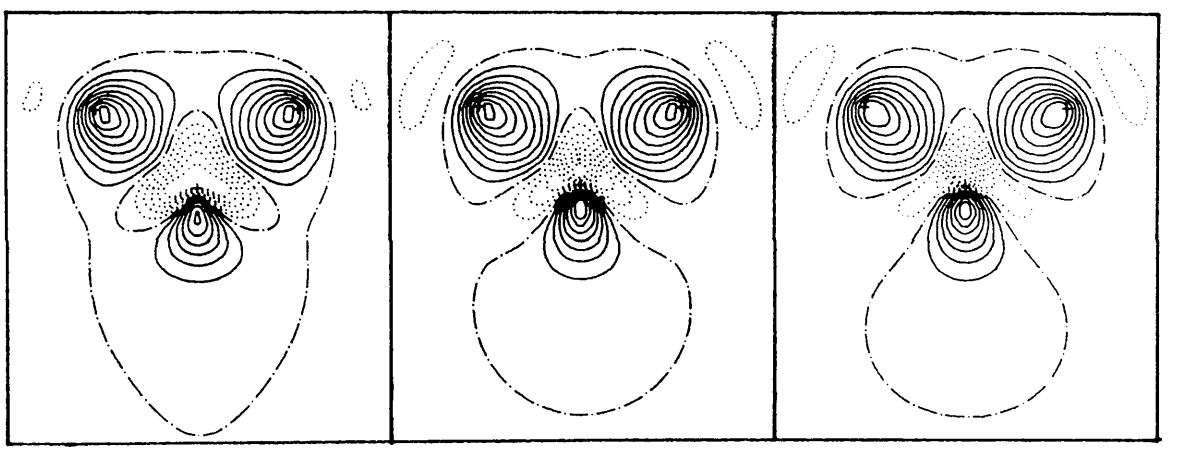

(*a*) (*b*) (*c*)

Fig. 5. Static difference-electron-density distribution of water from LSEXP refinements (Hirshfeld, 1977*a*), contour interval 0.1 e Å^{-3}, for structure factors (*a*) without thermal motion, (*b*) at 100 K, (*c*) at 300 K.

Table 2. *Coefficients in equation (A6)*

l	a_l	b_l
1	0.813589	0.088342
2	−3.575370	0.468548
3	8.045967	1.360815
4	−6.335496	12.893063

the electron-density distribution of N_2 is approximated by the sum of the electron-density distributions of two spherically averaged atoms. This leads to the expression for the scattering factor of N_2:

$$F_{N_2}(\mathbf{k}) = 2\cos(\mathbf{k}\cdot\mathbf{R}/2) f_N(|\mathbf{k}|/4\pi). \quad (A5)$$

Here f_N is the spherical atomic scattering factor. The scattering factor f_N calculated from atomic orbitals expanded in Slater functions is a rational function of $[(\sin\theta)/\lambda]^2$. To evaluate the integral in (A3) we approximate f_N by

$$f_N[(\sin\theta)/\lambda] = \sum_{l=1}^{4} a_l/\{b_l + [(\sin\theta)/\lambda]^2\}. \quad (A6)$$

The coefficients in (A6) (see Table 2) were fitted to the scattering-factor table of N taken from *International Tables for X-ray Crystallography* (1974). The fit is accurate to four significant figures. Combination of (A3) with (A4), (A5) and (A6) leads to

$$F_N(\mathbf{k}) = (1/\pi)\exp(i\mathbf{k}\cdot\mathbf{R}/2)\sum_{l=1}^{4} a_l \lim_{\varepsilon\to 0}\int \mathrm{d}\mathbf{u}\, i\delta(u_x)\delta(u_y) \times\cos[(\mathbf{k}-\mathbf{u})\cdot\mathbf{R}/2][b_l + (|\mathbf{k}-\mathbf{u}|/4\pi)^2]^{-1} \times(u_z + i\varepsilon)^{-1}. \quad (A7)$$

After integration over u_x and u_y this can be written as

$$F_N(\mathbf{k}) = (1/\pi)\exp(i\mathbf{k}\cdot\mathbf{R}/2) \times\sum_{l=1}^{4}\lim_{\varepsilon\to 0} a_l/[b_l + (|k|^2 - \varepsilon^2 + 2ik_z\varepsilon)/(4\pi)^2] \times\int \mathrm{d}u_z\{(2ik_z - iu_z - \varepsilon)/[(4\pi)^2 b_l + k_x^2 + k_y^2 + (k_z - u_z)^2] + (iu_z + \varepsilon)/(u_z^2 + \varepsilon^2)\} \times\cos[R(k_z - u_z)/2]. \quad (A8)$$

The integral in (A8) can be decomposed into six terms:

$$\int \mathrm{d}u_z\{i(k_z - u_z)/[(4\pi)^2 b_l + k_x^2 + k_y^2 + (k_z - u_z)^2]\} \times\cos[R(k_z - u_z)/2] = 0, \quad (A9.1)$$

$$\int \mathrm{d}u_z\{(ik_z - \varepsilon)/[(4\pi)^2 b_l + k_x^2 + k_y^2 + (k_z - u_z)^2]\} \times\cos[R(k_z - u_z)/2] = \pi(\varepsilon - ik_z)/[(4\pi)^2 b_l + k_x^2 + k_y^2]^{1/2} \times\exp\{-(R/2)[(4\pi)^2 b_l + k_x^2 + k_y^2]^{1/2}\}, \quad (A9.2)$$

$$\cos(Rk_z/2)\int \mathrm{d}u_z[iu_z/(u_z^2 + \varepsilon^2)]\cos(Ru_z/2) = 0, \quad (A9.3)$$

$$\cos(Rk_z/2)\int \mathrm{d}u_z[\varepsilon/(u_z^2 + \varepsilon^2)]\cos(Ru_z/2) = \pi\cos(Rk_z/2)\exp(-\varepsilon R/2), \quad (A9.4)$$

$$\sin(Rk_z/2)\int \mathrm{d}u_z[iu_z/(u_z^2 + \varepsilon^2)]\sin(Ru_z/2) = -i\pi\sin(Rk_z/2)\exp(-\varepsilon R/2), \quad (A9.5)$$

$$\sin(Rk_z/2)\int \mathrm{d}u_z[\varepsilon/(u_z^2 + \varepsilon^2)]\sin(Ru_z/2) = 0. \quad (A9.6)$$

Equations (A9.1), (A9.3) and (A9.6) vanish due to the odd parity of the integrand. Equations (A9.2) and (A9.4) follow from the cosine Fourier transform of $\exp(-|x|)$. Equation (A9.5) follows from the sine Fourier transform of $\mathrm{sign}(x)\exp(-|x|)$. After taking the limit as $\varepsilon\to 0$ and substituting (A6), one obtains the final result (with φ the angle between $\mathbf{k}$ and $\mathbf{R}$)

$$F_N(\mathbf{k}) = f_N[(\sin\theta)/\lambda] - \sum_{l=1}^{4} a_l i(\cos\varphi)(\sin\theta) \times\lambda\{b_l + [(\sin\theta)/\lambda]^2\}^{-1} \times\exp[-2\pi R(\{b_l + [(\sin\varphi)(\sin\theta)/\lambda]^2\}^{1/2} - i(\cos\varphi)(\sin\theta)/\lambda)] \times\{b_l + [(\sin\varphi)(\sin\theta)/\lambda]^2\}^{-1/2}. \quad (A10)$$

In Fig. 6 the result is plotted as function of $(\sin\theta)/\lambda$ for several values of φ. For $\varphi = 0°$, the curve is identical to the scattering-factor curve of the free spherical N atom. At higher values of φ the effect of the sharp boundary results in oscillating curves. The present treatment is easily extended to deformed or

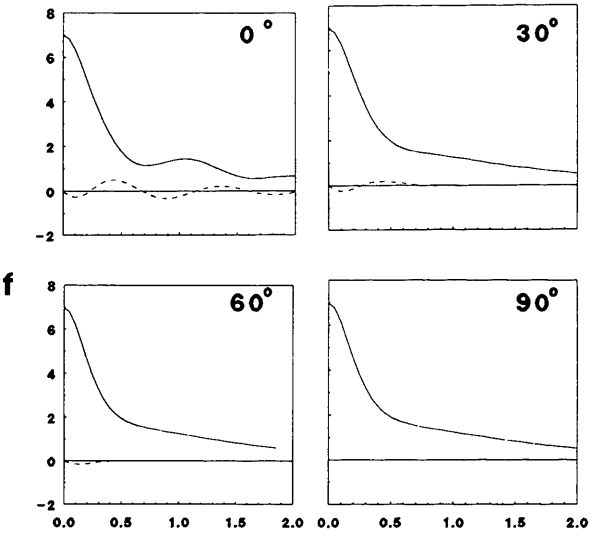

Fig. 6. Scattering factor according to the theory of Bader, Beddall & Cade (1971) of an atom in N_2 as a function of $(\sin\theta)/\lambda$ at four angles between $\mathbf{k}$ and the N–N axis: —— real part; - - - - imaginary part.

pseudo atoms in which the atomic electron-density distribution is written as the sum of the free atomic electron-density distribution plus an expansion into deformation functions with Slater-type orbital radial dependence.

References

ARFKEN, G. (1985). *Mathematical Methods for Physicists*, pp. 585, 694. New York: Academic Press.

BADER, R. F. W., BEDDALL, P. M. & CADE, P. E. (1971). *J. Am. Chem. Soc.* **93**, 3095-3107.

BAERENDS, E. J., ELLIS, D. E. & ROSS, P. (1973). *Chem. Phys.* **2**, 41-51.

BAERENDS, E. J. & ROSS, P. (1973). *Chem. Phys.* **2**, 52-59.

BAERENDS, E. J., VERNOOYS, P., ROOZENDAAL, A., BOERRIGTER, P., KRIJN, M. P. C. M., FEIL, D. & SUNDHOLM, D. (1985). *J. Mol. Struc.* **133**, 147-159.

ERIKSSON, A. & HERMANSSON, K. (1983). *Acta Cryst.* B**39**, 703-711.

HANSEN, N. K. & COPPENS, P. (1978). *Acta Cryst.* A**34**, 909-921.

HERMANSSON, K. (1983). *Chem. Phys. Lett.* **99**, 295-300.

HIRSHFELD, F. L. (1977*a*). *Isr. J. Chem.* **16**, 226-229.

HIRSHFELD, F. L. (1977*b*). *Theor. Chim. Acta*, **44**, 129-138.

International Tables for X-ray Crystallography (1974). Birmingham: Kynoch Press. (Present distributor Kluwer Academic Publishers, Dordrecht.)

KRIJN, M. P. C. M. & FEIL, D. (1988). *J. Chem. Phys.* **89**, 4199-4208.

KRIJN, M. P. C. M., GRAAFSMA, H. & FEIL, D. (1988). *Acta Cryst.* B**44**, 609-616.

MCWEENEY, R. (1951). *Acta Cryst.* **4**, 513-519.

RYSHIK, I. M. & GRADSHTEYN, I. S. (1965). *Table of Integrals, Series and Products*, p. 711. New York: Academic Press.

STEVENS, E. D., RYS, J. & COPPENS, P. (1977). *Acta Cryst.* A**33**, 333-338.

STEWART, R. F. (1976). *Acta Cryst.* A**32**, 565-574.

STEWART, R. F. (1980). *Electron and Magnetization Densities in Molecules and Crystals*, pp. 439-441. London: Plenum Press.

STEWART, R. F. & FEIL, D. (1980). *Acta Cryst.* A**36**, 503-509.

VELDERS, G. J. M. & FEIL, D. (1989). *Acta Cryst.* B**45**, 359-364.

Acta Cryst. (1992). A**48**, 872-879

A Stochastic Model for X-ray Diffraction from Imperfect Crystals

BY T. J. DAVIS

CSIRO Division of Materials Science and Technology, Locked Bag 33, *Clayton, Victoria* 3168, *Australia*

(*Received* 6 *January* 1992; *accepted* 27 *April* 1992)

Abstract

A model of crystal defects is developed to describe the diffraction of X-rays from imperfect crystals containing defect surfaces and crystal grains. The model, which is based on continuum theory for an isotropic homogeneous elastic medium, leads to a stochastic first-order differential equation, known as a Langevin equation. The solution of this equation is used to derive a correlation function for the strain-dependent term in the formula for the crystal reflectance. A consequence of the model is that the kinematic reflectivity of an imperfect crystal is given by the convolution between the perfect-crystal reflectivity and a function that transforms between a Gaussian and a Lorentzian depending on a correlation length in the crystal.

Introduction

X-ray rocking curves obtained from thin crystalline films or superlattices may show complicated features that are characteristic of the correlations between the crystal structures in the films. However, in the presence of defects causing severe distortions, many of the features are lost and the result is usually a broad Gaussian-like curve, the width of which is taken as a measure of the quality of the crystal. The loss of structure in the rocking curve can be interpreted as a loss of information about the nature of the crystal, which suggests that it should be possible to model such a curve with only a few parameters. For example, the theory of X-ray diffraction by Zachariasen (1967) only involves the size of the mosaic-crystal grains and the half-width of the distribution function for the grain orientations. The statistical theories of X-ray diffraction by Kato (1980) and Becker & Al Haddad (1990) contain two correlation lengths that relate to the statistical nature of the crystal imperfections.

Davis (1991) suggested that a first-order stochastic differential equation could model the effects of a class of crystal imperfections on the strain-dependent term in the equation for the crystal reflectance. This model was used to derive a partial differential equation describing dynamical diffraction in a crystal containing point-like defects and crystal grains that are misoriented with respect to the perfect lattice.

In this paper, the first-order stochastic equation is derived from continuum theory for a homogeneous isotropic elastic solid containing defects. This equation is related to the Markov process used by Becker & Al Haddad (1989) to derive an order parameter for their dynamical theory and it involves parameters similar to those in the mosaic-crystal theory of Darwin, as used by Zachariasen (1967). The solution

0108-7673/92/060872-08$06.00